*Egypt. J. Chem.* **Vol. 66**, No. 2 pp. 385 - 393 (2023)

**Egyptian Journal of Chemistry**

**http://ejchem.journals.ekb.eg/**

# Design ,Synthesis, Insilco Study and Biological Evaluation of New Coumarin-Oxadiazole Derivatives as Potent Histone Deacetylase Inhibitors

**Sarah Sattar Jabbar [a*], Mohammed Hassan Mohammed [b]**

[a,b] *Department of Pharmaceutical Chemistry, College of Pharmacy, University of Baghdad/Iraq*

**Abstract**

A new series of HDAC inhibitors were designed, synthesized, bearing acyl semicarbazide, hydrazide and hydrazide derivatives as ZBGs, alkyl thio oxadiazole as the linker group and coumarin as the cap group .These derivatives were evaluated for their HDACs inhibitory activities against MDA-MB-231 (a human breast cancer cell line) and HepG2 (a human hepatocellular carcinoma cell line), most of them had substantial HDAC inhibitory action and displayed better inhibitory activities against HepG2 cell line than against MDA-MB-231 cell line .Compound F5 was found to be the most powerful HDAC inhibitor, with an IC50 of 17.92, 20.72 µg/ml which were better than that of SAHA's with IC50 = 39.84, 36.52 µg/ml against MDA-MB-231 and HepG2 cell lines respectively. Compounds F1 with IC50 of 30.21, 30.07 µg/ml, compounds F2 with IC50 of 31.59, 26.27 µg/ml and compounds F4 with IC50 of 39.60, 31.40 µg/ml higher than that of SAHA's with IC50 = 39.84, 36.52 µg/ml against MDA-MB-231 and HepG2 cell lines respectively. The probable binding modes of compounds into HDAC enzymes (HDAC1 and 2) is deducted by the docking study which provided a rationale for the greatest -inhibitory activity. These findings suggested that these compounds could be a good option for developing novel HDAC inhibitors with anticancer properties.

Keywords: cancer; epigenetic modification; histone deacetylase inhibitors; coumarine; oxadiazole; hydrazide.

## Introduction

Cancer is one of the major causes of death worldwide. Despite advances in new chemotherapeutic agents that restriction out of uncontrolled cell division processes for the treatment of various malignancies, significant side effects and drug resistance continue to be one of the predominant limitations. Different research are being conducted in order to uncover and develop effective anticancer drugs [1].

The risk of cancer formation may be enhanced by epigenetic silencing of certain genes, resulting in unrestrained cell growth [2].

Recent research has shown inappropriate epigenetic alterations such as inappropriate DNA methylation, histone changes, nucleosome abnormalities, and non-coding RNAs as Epigenetic mechanisms all been linked to the initiation and progression of cancer [3].

One of the key mechanisms is an inappropriate histone modification, among them acetylation is the primary mechanism under investigation [4]. acetylation regulates by two groups of enzymes, histone acetyltransferase (HATs) that catalyze the transfer of acetyl groups to histone amino-terminal lysine residues likely to result in local chromatin expansion and greater accessibility of regulatory proteins to DNA [5], whereas histone deacetylase (HDACs) that catalyze the removal of acetyl groups likely to result in chromatin compaction and transcriptional suppression [4].

Several studies show that some members of the histone deacetylase (HDAC) family are abnormally expressed in a variety of cancers and play a non-redundant role in regulating malignant cell parameters. Consequently, overexpression of histone deacetylase (HDAC) activity, histone tail deacetylation and chromatin architecture all have a significant correlation. Certain genes may become transcriptionally inaccessible to transcription factors, resulting in their suppression. This could be a mechanism to silence tumor suppressor genes like p53 and cyclin-dependent kinase inhibitor genes like p21[6].

*Corresponding author e-mail: ph.sarahsattar@gmail.com
Receive Date: 16 April 2022, Revise Date: 29 May 2022, Accept Date: 30 May 2022
DOI: 10.21608/EJCHEM.2022.134043.5912

HDACs are involving in a variety of biological processes that include the cell cycle control, autophagy, metabolism, apoptosis, DNA repair, senescence, and chaperone function. Human HDACs with eighteen different isoforms are split into four groups, class I HDACs (HDACs 1, 2, 3, and 8) are associated to RPD3 deacetylase [7] and class II HDACs are divided into two subclasses: class IIa (HDACs 4, 5, 7, and 9) and class IIb (HDACs 6 and 10) [8]. The yeast silent information regulator 2 (Sir2) family is homologous to the class III HDACs (SIRT1 through SIRT7) [9]. The class IV HDAC contains only one member (HDAC11). Class I, II, and IV HDACs similarly require Zn2+ for catalytic activity and also known as classical HDACs, most of them share a highly conserved deacetylase domain, however, class III HDACs has a unique catalytic mechanism that requires the cofactor $NAD^+$[10].

The zinc dependent HDACs classes have been extensively studied and subjected to inhibition studies as a cancer therapeutic strategy [11].

In spite of the huge structural variety, classical HDACs inhibitor have the universal pharmacophore model consists of three parts [12]– [15]: 1) a zinc binding group (ZBG) chelating with zinc ion at the bottom of active site of HDACs as hydroxyl amine, thiourea, thiol, amide or biguanide [16]– [19]; 2) a cap group, generally a hydrophobic ring interacting with the amino acids at the entrance of HDACs. The cap group can adopt extensive structural variation as coumarin [12], [20],[21], making it possible to design HDAC inhibitors with great variety of structures [22]; 3) a linker connecting the ZBG and the cap group, such as alkyl oxadiazole [23]– [25]. The selectivity and potency in these different inhibitors rely upon varieties in any or all of the three domains. Accordingly, new zinc dependent HDAC inhibitors should have met these three requirements [26].

**Materials and Methods**

Chemicals supplied by hyper-chem (China) were used, Thin-layer chromatography (TLC) was employed to monitor reaction completion and verify compound purity using aluminum sheets pre-coated with Silica gel GF254 (type 60) and subjected to UV-254 nm. The Stuart SMP3 melting point device was used to detect melting points in open capillary tubes. Spectroscopic analysis, Fourier-transform Infrared (FTIR) at Baghdad University-College of Pharmacy using Shimadzu IRAffinity-1 Spectrometer (Shimadzu, Japan) and Specac® Quest ATR-diamond type (UK)). Proton nuclear magnetic resonance ($^1$HNMR) and Cytotoxicity assay both were performed at the University of Tehran, Islamic Republic of Iran using MDA-MB-231 and HepG2 cell lines were obtained from the Pasteur Institute (Tehran, Iran). Molecular docking studies was performed using Molecular Operating Environment (MOE) software version 2015.10 (Chemical Computing Group, Montreal, Canada).

**Chemical synthesis**

The overall synthetic pathways of the final compounds are shown in (**scheme 1)**.

**Synthesis of 2-oxo-2H-chromene-3-carbohydrazide (II).**

In 25 ml DMF, Coumarin-3-carboxylic acid compound I (2.5 g, 13.15 mmole) was dissolved, and HOBt (2 g, 15.78 mmole) was added in one portion followed by EDC.HCl (3 g, 15.78 mmole). The mixture was stirred at room temperature, the activation of the carboxylic acid group and the formation of active HOBt ester was checked by TLC. The resulting activated HOBT ester was then slowly added by inverse addition to 12.5 ml DMF containing hydrazine 99.9% (1.3 ml, 26.3 mmole) and cyclohexene (0.5ml) while the temperature was kept at $0^0$C, then the reaction mixture was stirring for 2 day at room temperature that monitored by TLC. The product was obtained by the addition of 100 ml of cold distilled water, filtration then excessive washing with distilled water and sodium carbonate 5%, recrystallized with ethanol to get compound II as pale –yellowish crystal [27]; m.p: 207-209$^0$C; yield 70%; FT-IR (ATR; υ,cm$^{-1}$): 3302 (NH, hydrazide), 3220,3208 ($NH_2$, hydrazide), 1701 (C=O, coumarin), 1662 (C=O, hydrazide); $^1$HNMR (500 MHz, DMSO-d6), ppm : 4.28 (s, 2H, $NH_2$, $CONHNH_2$ ), 7.47-7.78 (m, 4H, Ar-H) , 8.38 (s, 1H, H-4, coumarin), 9.28 (s, 1H, NH, $CONHNH_2$).

**Synthesisof3-(5-mercapto-1,3,4-oxadiazol-2-yl)-2H-chromen-2-one) (III).**

In 40 ml absolute ethanol, compound II (1g, 4.9 mmole) was dissolved, carbon disulphide (0.3 ml, 4.9 mmole) and potassium hydroxide (0.28 g, 4.9 mmole) were added at $0^0$C then the reaction mixture was refluxed until the evolution of $H_2S$ gas ceased. Excess solvents were evaporated, and the residue was dissolved in water, then acidified with 5 % dilute hydrochloric acid to pH 4-5. The precipitate was filtered off, dried and crystallized from ethanol to give compound III as dark-yellow solid[28]; m.p: 178-181$^0$C; yield 85%; FT-IR (ATR;υ,cm$^{-1}$): 1697 (C=O, coumarin), 1616,1570, (2C=N, oxadiazole), 1269 (C=S), 1033 (C–O–C, oxadiazole); $^1$HNMR (500 MHz, DMSO-d6): ppm, 7.39–7.77 (m, 4H, Ar–H), 8.32 (s, 1H, H-4, coumarin),14.02 (s, 1H, SH).

**Synthesis of 3-(5-((5-oxoheptyl) thio)-1,3,4-oxadiazol-2-yl)-2H-chromen-2-one (IV).**

In 50ml dry DMF, compound III (0.5 g, 22.3 mmole) was dissolved, $K_2CO_3$ (0.15 g, 11.15 mmole) was added with stirring for 5-10 min, a white ppt. was formed, then 5- bromoethylvalerate (0.33 ml, 22.3 mmole) was added, the reaction mixture was stirring gently overnight at room temperature, monitored by TLC. Then cold D.W was added and the formed ppt. was filtered, washed with D.W and n-hexane then dried and recrystallized from ethanol to give compound IV as light beige solid [29]; yield 95%; m.p: 221-223$^0$C; FT-IR (ATR; υ, cm$^{-1}$): 1720 (C=O, aliphatic ester), 1701(C=O, coumarin), 1666,1620 (2C=N, oxadiazole), 1033 (C–O–C, oxadiazole); $^1$HNMR (500 MHz, DMSO-d6): ppm, 1.17(t, 3H, aliphatic$CH_3$-$CH_2$-C(O)-), 1.63 (m, 2Haliphatic -$CH_2$-$CH_2$-C(=O)- and 2H, S-$CH_2$-$CH_2$-), 2.36 (t, 2H aliphatic -$CH_2$-C(=O)-) , 3.17 (t, 2H, -S-$CH_2$-), 4.02 (t, 2H, aliphatic-O-CH2-CH3), 7.31–7.68 (m, 4H, Ar–H), 8.39 (s, 1H, H-4, coumarin).

**Synthesisof2-(5-((5-(2-oxo-2H-chromen-3-yl)-1,3,4-oxadiazol-2 yl)thio)pentanoyl)hydrazine-1-carboxamide(F1).**

In 20 ml absolute ethanol, Semicarbazide.HCl (0.12 g, 1.116 mmole) and triethylamine (0.12 ml, 1.116 mmole) were mixed and stirred for few minutes, then an absolute ethanolic solution 20 ml containing compound (IV) (0.4 g, 1.116 mmole) was added gradually then stirred for 12 hour at room temperature, the precipitate was formed, filtered and washed with ethanol, and left to dry to give compound F1 as a light green solid[30]; m.p: 265-268$^0$C; yields 80 %; FT-IR (ATR; υ, cm$^{-1}$): 3464 (NH, hydrazide), 3217,3147 ($NH_2$, hydrazide), 1701 (C=O, coumarin), 1681 (C=O, hydrazide), 1608,1585 (2C=N, oxadiazole), 1049 (C–O–C, oxadiazole); $^1$HNMR (500 MHz, DMSO-d6): ppm, 1.67(m, 2H, aliphatic -$CH_2$-$CH_2$-C(=O)- and 2H, S-$CH_2$-$CH_2$), 2.88 (t, 2H, aliphatic -$CH_2$-C(=O)-), 3.36 (t, 2H, -S-$CH_2$-), 6.76 (s, 1H, $NH_2$, urea), 7.18–7.68 (m, 4H, Ar–H), 8.31(s, 1H, H-4, coumarin),9.95 (s, 1H, NH, urea), 10.87 (s, 1H, NH, urea).

**Synthesis of 5-((5-(2-oxo-2H-chromen-3-yl)-1,3,4-oxadiazol-2-yl) thio)pentanehydrazide (F2).**

In 80 ml absolute ethanol, compound IV (1 g, 1.34 mmole) was dissolved, and hydrazine hydrate 99.9% (0.28 ml,2.68 mmole) was added, left to stirring for 24 hrs. at room temperature. The mixture was filtered and washed with chloroform to get compound F2 as pale- yellowish green solid[31]; m.p: 259-261$^0$C; yield 50%; FT-IR (ATR; υ, cm$^{-1}$) : 3390 (NH, hydrazide), 3232,3194 ($NH_2$, hydrazide), 1693 (C=O, coumarin), 1662 (C=O, hydrazide), 1624 ,1608 (2C=N, oxadiazole), 1033 (C–O–C, oxadiazole); $^1$HNMR (500 MHz, DMSO-d6): ppm, 1.66 (m, 2H, aliphatic -$CH_2$-$CH_2$-C(=O)- and 2H, -S-$CH_2$CH2), 2.46 (t, 2H, aliphatic -$CH_2$-C(=O)-), 3.28 (t, 2H, -S-$CH_2$-), 4.14 (s, 2H, $NH_2$, $CONHNH_2$), 7.33–7.80 (m, 4H, Ar–H), 8.31 (s, 1H, H-4, coumarin), 8.70 (s, 1H, NH, $CONHNH_2$).

**Synthesis of N'-acetyl-5-((5-(2-oxo-2H-chromen-3-yl)-1,3,4-oxadiazol-2-yl) thio)pentanehydrazide(F3).**

In 100 ml flat bottom flask on an ice bath, Compound F3 was synthesized by dissolving compound F2 (0.4g,1.11mmole) in 30ml dry chloroform, triethylamine (0.15 ml, 1.11 mmole) was added slowly with continuous stirring then acetyl chloride (0.16 ml, 2.22 mmole) was added by simultaneous drop by drop, after that the stirring was continued overnight at room temperature. The product was obtained by evaporating some of the solvent volume, filtered and rinsed with distilled water to give compound F3 as light –green solid[32]; m.p: 268-270$^0$C; yield 70%; FT-IR (ATR; υ, cm$^1$): 3277 (NH, hydrazide), 1701 (C=O, coumarin), 1671 (C=O, hydrazide), 1620,1608 (2C=N, oxadiazole), 1033 (C–O-C, oxadiazole); $^1$HNMR (500 MHz, DMSO-d6): ppm, 1.70 (m, 2H, aliphatic -$CH_2$-$CH_2$-C(=O)- and 2H, S-$CH_2$-CH2-), 1.98 (t, 3H, aliphatic –$CH_3$-C(=O)-), 2.24 (t, 2H, aliphatic -$CH_2$-C(=O)-) , 3.28 (t, 2H, -S-$CH_2$-), 7.39–7.78 (m, 4H, Ar–H), 8.28 (s, 1H, H-4, coumarin), 9.01,9.58 (s, 1H, NH, CONHNH) respectively.

**Synthesis of N-(2-chloroacetyl)-5-((5-(2-oxo-2H-chromen-3-yl)-1,3,4-oxadiazol-2-yl) thio)pentanehydrazide(F4).**

In 30ml dry chloroform on an ice bath, Compound F4 was synthesized by dissolving compound F2 (0.4 g, 1.11 mmole), triethylamine (0.15 ml, 1.11 mmole) was added drop by drop with continuous stirring then chloro-acetyl chloride (0.18 ml, 2.22 mmole) was added slowly after that the stirring was continued overnight at room temperature. The product was obtained by evaporating some of the solvent volume, filtered then rinsed with distilled water to give compound F4 as off white-solid[32]; yield 60%; m.p: 273-275; FT-IR (ATR; υ, cm$^{-1}$): 3263 (NH, hydrazide), 1697 (C=O, coumarin) , 1688 (C=O, hydrazide), 1624,1608 (2C=N, oxadiazole), 1033 (C–O–C, oxadiazole); $^1$HNMR (500 MHz, DMSO-d6): ppm, 1.68 (m, 2H, aliphatic –$CH_2$-$CH_2$-C(=O)- and 2H, -S-$CH_2CH_2$), 2.21 (t, 2H, aliphatic -$CH_2$-C(=O)-) ,3.14 (t, 2H, -S-$CH_2$-), 4.0(s, 2H, C(=O)-$CH_2$-Cl), 7.39–7.77 (m, 4H, Ar–H),8.21 (s,

1H, H-4,coumarin), 9.18,9.41 (s, 1H, NH, CONHNH) respectively.

**Synthesis of 1-(triethylammonio) 2-(5-((5-(2-oxo-2H-chromen-3-yl)-1,3,4-oxadiazol-2-yl)thio) pentanoyl) hydrazine-1-carbodithioate(F5).**

In 20 ml dry THF, compound F2 (0.4 g, 1.11 mmole) was dissolved, cooled to 0°C, then treated with triethyl amine (0.15 ml, 1.11 mmole) and stirring for 30 min. $CS_2$ (0.11 ml, 2.22 mmol) then was added and the mixture was stirred for 12 hrs. at room temperature. The product was precipitated from THF by $Et_2O$ to give compound F5 as light green solid [33]; m.p: 293-295; yield 73%; FT-IR (ATR; υ, $cm^{-1}$): 3267 (NH, hydrazide), 1701 (C=O, coumarin), 1679 (C=O, hydrazide), 1624,1608 (2C=N, oxadiazole), 1033 (C–O–C, oxadiazole); $^1$HNMR (500 MHz, DMSO-d6): ppm, 0.92 (t, 3H ,-N-$CH_2$-$CH_3$-), 1.47(q, 2H, -N-$CH_2$-$CH_3$), 1.65 (m, 2H, aliphatic -$CH_2$-$CH_2$-C(=O)- and 2H, S-$CH_2$-$CH_2$), 2.36 (t, 2H, aliphatic -$CH_2$-C(=O)-) , 3.14 (t, 2H, -S-$CH_2$-) , 6.97–7.68 (m, 4H, Ar–H), 7.67(s, 1H, NH, amide), 8.39 (s, 1H, H-4, coumarin),11.3 (s, 1H, NH, thioamide).

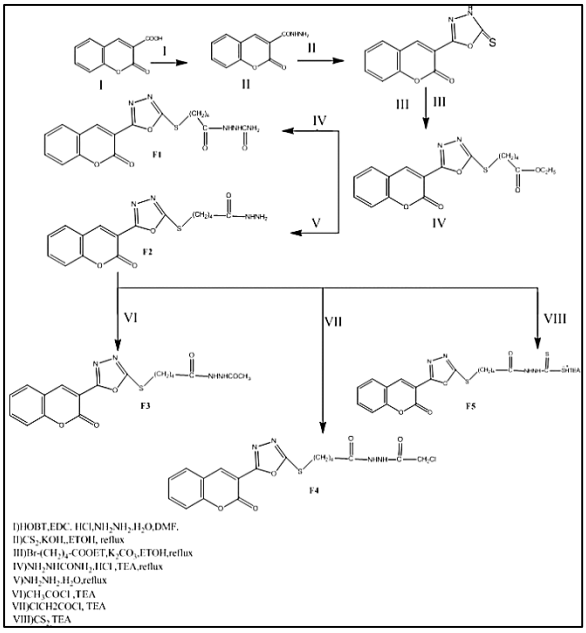


**Scheme 1.** Synthesis of the target compounds (F1-F5)

**In vitro Cytotoxicity Assay**

*In vitro* cytotoxicities of compound (F1-F5) were assessed using the MTT assay. Two cell lines that overexpress HDACs, human hepatic carcinoma (HepG2) and human breast cancer cell line (MDA-MB-231) were employed. The assay findings were presented as a mean of three independent tests, with IC50s calculated to indicate the efficiency of the investigated compounds in inhibiting the proliferation of the two cell lines.

**Insilco Docking Study**

The Molecular Operating Environment (MOE) software version 2015.10 was used to conduct the docking studies (Chemical Computing Group, Montreal, Canada). HDAC1 ( (PDB code 5ICN) [16]and HDAC2 (PDB code4LXZ)[34]). X-ray crystal structures were retrieved from the Protein Data Base (PDB). All water molecules were removed from PDB files, and hydrogen atoms were then added to the protein. The MOE-Dock algorithm was then used to dock the optimized shape of the chemical into the binding site. The London dG was selected as initial scoring method and the Rigid Receptor was selected as the final scoring method. The best 5 poses of each ligand were retained and scored. Finally, the geometry of docked complex was analyzed by the pose viewer utility in MOE.

## Results and Discussion

**Chemical Synthesis**

**Compound II** was obtained as hydrazide, the process includes the activation of the carboxylic acid by HOBt, EDC-HCl to get HOBt esters then the hydrazinolysis of HOBt esters. The IR spectrum shows a shifting of C=O absorption from 1735 to 1662 $cm^{-1}$ and new bands at 3315,3201,3228$cm^{-1}$ related to (NH, $NH_2$ stre.). $^1$HNMR shows the appearance of new signals related to $CONHNH_2$ protons at 9.28 and 4.28 ppm. respectively, and both as a singlet.

**Compound III** was prepared by synthesis of the oxadiazole nucleus by refluxing an ethanolic suspension of hydrazide with $CS_2$ in the presence of (KOH). The IR spectrum and $^1$HNMR shows disappearance of all bands related to hydrazide group and the appearance of signal related to SH at 14.02 as singlet.

**Compound IV** was prepared by a nucleophilic substitution ($SN_2$) reaction between compound III and 5- bromoethylvalerate in dry DMF and in the presence of anhydrous potassium carbonate as a catalyst. The IR spectrum shows the appearance of new bands at 1720$cm^{-1}$ (C=O, aliphatic ester) and new bands at 2873,2947,2985(CH stre., $(CH_2)_4$, $CH_3$) which were a clue for S-alkylation. $^1$HNMR shows the presence of new signals at 1.17 (t, 3H, $COCH_2CH_3$), 1.63 (m, 2H, aliphatic -$CH_2$-$CH_2$-C(O)- and 2H, S-$CH_2CH_2$), 2.36 (t, 2H, aliphatic -$CH_2$-C(=O)-), 4.03 (q, 2H, $COOCH_2CH_3$), and the absence of SH signal at 14.02 and instead of the appearance

of new signal at 3.17 ppm which was related to –$SCH_2$.

**Compound F1** was prepared by the reaction of ethyl ester of compound IV with semicarbazide.HCl. The IR spectrum shows a shifting of C=O absorption from 1720 to 1689 $cm^{-1}$ due to the conversion of ester to acyl semicarbazide, show appearance new bands at 3155, 3197,3464 $cm^{-1}$ ($NH_2$, NH stre., urea). $^1$HNMR shows the appearance of signals were related to $CONHNHCONH_2$ at 6.76, 9.95,10.87 ppm. ($NH_2$, NH, urea) respectively all of them as singlet.

**Compound F2** was prepared by the hydrazinolysis of ethyl ester of compound IV. The IR spectrum shows shifting of C=O absorption from 1720 to 1662 $cm^{-1}$ due to the conversion of ester to hydrazide, the appearance characteristic bands at 3390,3232,3194 $cm^{-1}$ which were related to (NH, $NH_2$ stre., $CONHNH_2$). $^1$HNMR shows the substitution of ester protons at 1.17,4.03 ppm. by new protons at 4.14 and 8.7 ppm. related to ($CONHNH_2$) both as a singlet.

**Compound F3** was prepared by N-acytalation of compound F2 using acetyl chloride. The IR spectrum shows band at 1671 (C=O, hydrazide) and disappearance of 2 bands of $NH_2$ stre., of hydrazide F2. $^1$HNMR shows the appearance of new signals related to $CONHNHCOCH_3$ protons at 9.01, 9.58 (NH, amide) respectively both as a singlet and at 1.98 (3H, $–CH_3$-C(=O)-) as triplet.

**Compound F4** was prepared by N-acytalation of compound F2 using chloroacetylchloride. The IR spectrum shows a band at 1688 $cm^{-1}$ (C=O, hydrazide) and disappearance of 2 bands of $NH_2$ stre., of hydrazide F2. $^1$HNMR shows the appearance of the signals were related to $CONHNHCOCH_2Cl$ protons at 9.18,9.41 and 4.00 ppm. respectively all of them as a singlet.

**Compound F5** was prepared by reacting compound F2 with carbon disulfide as the sulfur source usually under basic conditions. The IR spectrum shows band of C-N str. at 1346 $cm^{-1}$, band of C=S str.at 1153 ,1033 $cm^{-1}$ and at 968 $cm^{-1}$ of C-S str.$^1$HNMRshows the signals were related to $CONHNHCS_2N(CH_2CH_3)_3$ protons at 7.67, 11.3 ppm. (NH, CONHNH) respectively both as a singlet and at 0.92 (q, 2H, N-$CH_2CH_3$), 1.47(t, 3H, N-$CH_2CH_3$).

**Cytotoxicity study**

At micromolar concentrations (6.25, 12.5, 25, 50, 100 µM), compounds F1-F5 were tested for their in vitro antiproliferative activity against two cancer cell lines, MDA-MB-231 (a human breast cancer cell line) and HepG2 (a human liver cancer cell line). The IC50s were measured to display the growth inhibitory effect of these compounds on the two cell lines table (1). Figures 1 and 2 show the cell viability percent of compounds F1- F5 comparable to SAHA against selected cell lines, inhibition of growth increases in a continuous and parallel manner as the concentration is increased.

| Sample | IC50 (µg/ml) | |
|---|---|---|
| | MDA-MB-231 | HepG2 |
| F1 | 31.5981 | 26.27572 |
| F2 | 30.21784 | 30.07824 |
| F3 | 61.6697 | 43.47328 |
| F4 | 39.6076 | 31.40249 |
| F5 | 17.92197 | 20.72367 |
| Saha | 39.8484 | 36.52026 |

**Table 1.** IC50 values of target compounds F1-F5**.**

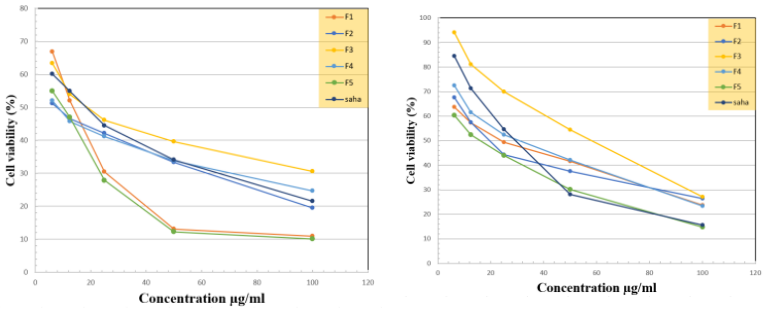


**Figure 1.** Comparative Concentration-cell viability percent curve of the target compounds (A): the cytotoxicity of compound F1-F5 against hepatic carcinoma cells, HepG2. (B): the cytotoxicity of compound F1-F5 against

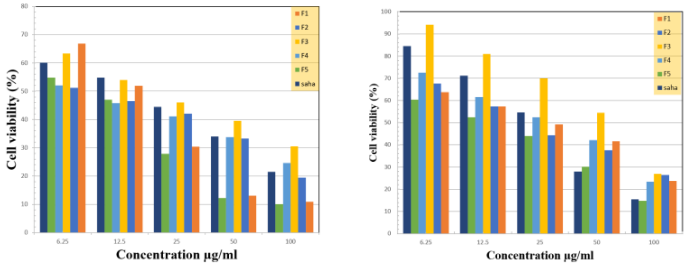


human breast cancer cell line, MDA-MB-231.

**Figure 2.** Comparative Histogram showing the concentration-cell viability percent of the tested compounds (A): the cytotoxicity of compound F1-F5 against hepatic carcinoma cells, HepG2. (B): the cytotoxicity of compound F1-F5 against human breast cancer cell line, MDA-MB-231.

Most of target compounds had substantial HDAC inhibitory action. Compound F5 was found to be the most powerful HDAC inhibitor, with an IC50 of 17.92, 20.72 µg/ml which were better than that of SAHA's with IC50 of 39.84, 36.52 µg/ml against MDA-MB-231 and HepG2 cell lines respectively. Figure 3 and 4 (captured at the IC50s) shows the difference in the magnitude of cytotoxicity between the compounds.

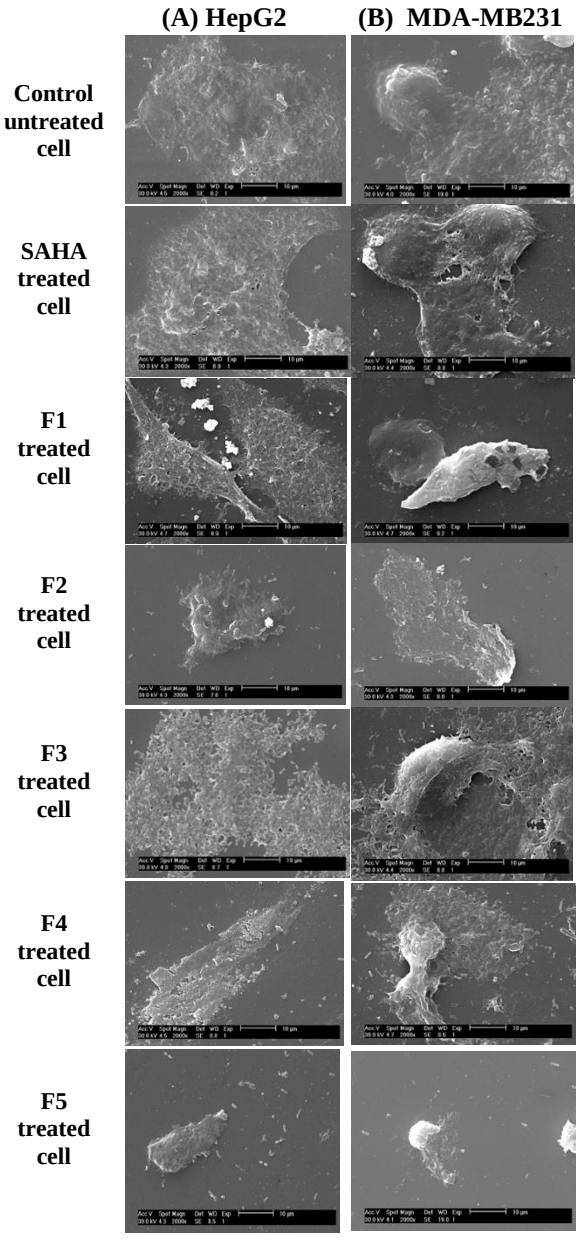


**Figure 3.** Morphology of the cell lines after treatment with compounds (F1-F5) at the IC50(A): HepG2(B): MDA-MB-231. Scale bar is 10µm.

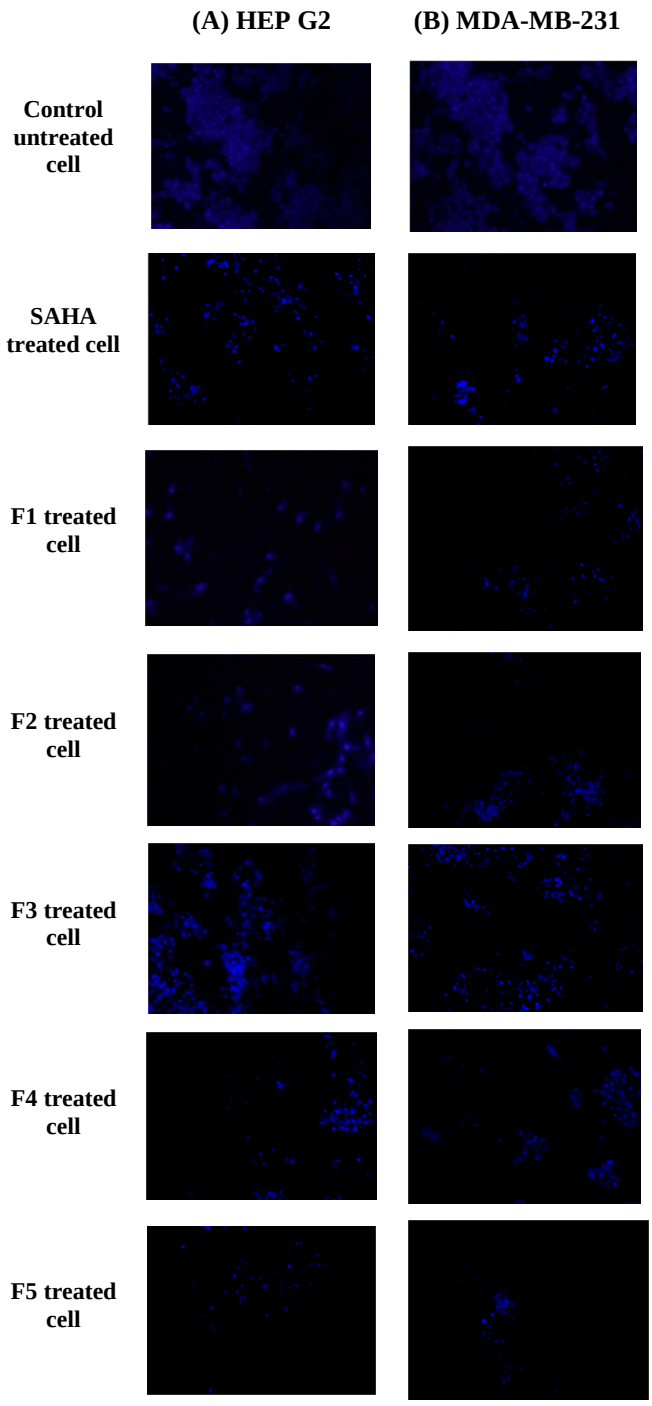


**Figure 4.** fluorescent images of selected cell lines, DAPI staining was used for labeling the nuclei. (A): HepG2 (B): MDA-MB-231

**Insilco study**

For comparison purposes, Compounds F1-F5 together with SAHA were docked against HDAC1 (PDB code: 5ICN) and HDAC2 (PDB code: 4LXZ), molecular docking studies were performed using the software MOE2015.10. *In vitro* cytotoxicities results agreed with molecular docking studies, which provided a rationale for the greatest inhibitory activity. Docking studies showed that compounds F1-F5 have binding affinities, hydrogen bond interactions between the ligand and the enzyme and distance of heteroatom from $Zn^{+2}$ better than, that of SAHA with selected isoform. The results of docking with these isoforms are summarized in Table 2. Images in figure 5 representing the occupation of the binding pocket of HDAC isoforms by target compounds and SAHA.

| Isoform /PDB code | ligand | Energy of Binding(Kcal/ mol) | Hydrogen bonds | Coordinating bond length (with zinc) [Å] |
|---|---|---|---|---|
| | SAHA | -8.07 | GLY 149(3.13 Å) | 2.13 |
| | F1 | -9.16 | GLY 149(3.22 Å), CYS 151(4.25 Å),HIS 141(2.83 Å) | 2.01 |
| | F2 | -8.06 | 2 H-bond with GLY 149(3.24and 3.11 Å ) | 2.07 |
| | F3 | -9.93 | TYR 303(2.81 Å) | 2.14 |
| | F4 | -9.28 | GLY 149(3.21 Å) | 2.09 |

**Table2.** Docking results of compound F1- F5 and SAHA against HDAC1 and 2.

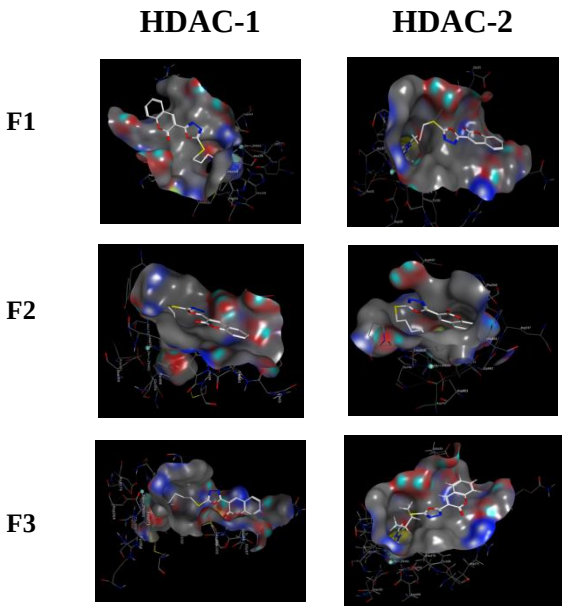


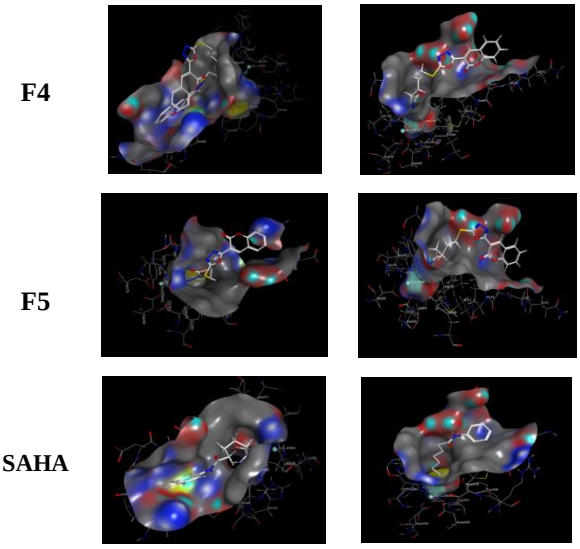


**Figure 5.** The occupation of the binding pocket of HDAC isoforms by target compounds and SAHA.

**Conclusion**

In the field of antitumor research, HDAC inhibitors have been found as potential anticancer agents. A new series of HDAC inhibitors was designed, synthesized, and their inhibitory effects were assessed in vitro experiments to obtain enhanced anticancer efficacy. Most compounds inhibited the hepatocellular carcinoma cell line HepG2 more effectively than the human breast cancer cell line MDA-MB-231. HDAC isoforms are effectively inhibited by compound F5. All of these findings suggest that these novel HDAC inhibitors could be attractive options for future anticancer drug development.

**Conflicts of Interest:** The authors declare no conflict of interest.

**Funding:** This research received no external funding.

**References**

[1] E. K. Akkol, Y. Genç, B. Karpuz, E. Sobarzo-Sánchez, and R. Capasso, "Coumarins and coumarin-related compounds in pharmacotherapy of cancer," *Cancers (Basel).*, vol. 12, no. 7, pp. 1–25, 2020, doi: 10.3390/cancers12071959.

[2] A. Lahm *et al.*, "Unraveling the hidden catalytic activity of vertebrate class IIa histone deacetylases," vol. 104, no. 44, pp. 17335–17340, 2007.

[3] S. Sharma, T. K. Kelly, and P. A. Jones, "Epigenetics in cancer," *Carcinogenesis*, vol. 31, no. 1, pp. 27–36, 2009, doi: 10.1093/carcin/bgp220.

[4] J. E. Bolden, M. J. Peart, and R. W. Johnstone, "Anticancer activities of histone deacetylase inhibitors," *Nat. Rev. Drug Discov.*, vol. 5, no. 9, pp. 769–784, 2006, doi: 10.1038/nrd2133.

[5] S. B. Baylin, J. H. Medicine, and J. E. Ohm, "FOCUS ON BIOM Epigenetic gene silencing in cancer – a mechanism for early oncogenic pathway addiction," no. March, 2006, doi: 10.1038/nrc1799.

[6] G. Giannini, W. Cabri, C. Fattorusso, and M. Rodriquez, "Histone deacetylase inhibitors in the treatment of cancer: Overview and perspectives," *Future Med. Chem.*, vol. 4, no. 11, pp. 1439–1460, 2012, doi: 10.4155/fmc.12.80.

[7] C. Micelli and G. Rastelli, "Histone deacetylases: Structural determinants of inhibitor selectivity," *Drug Discov. Today*, vol. 20, no. 6, pp. 718–735, 2015, doi: 10.1016/j.drudis.2015.01.007.

[8] S. A. Shinsky and D. W. Christianson, "Polyamine Deacetylase Structure and Catalysis: Prokaryotic Acetylpolyamine Amidohydrolase and Eukaryotic HDAC10," *Biochemistry*, vol. 57, no. 22, pp. 3105–3114, 2018, doi: 10.1021/acs.biochem.8b00079.

[9] L. L. Delehanty, G. C. Bullock, and A. N. Goldfarb, "Protein kinase D-HDAC5 signaling regulates erythropoiesis and contributes to erythropoietin cross-talk with GATA1," *Blood*, vol. 120, no. 20, pp. 4219–4228, 2012, doi: 10.1182/blood-2011-10-387050.

[10] H. M. Gao, J. Jiang, B. Wilson, W. Zhang, J. S. Hong, and B. Liu, "Microglial activation-mediated delayed and progressive degeneration of rat nigral dopaminergic neurons: Relevance to Parkinson's disease," *J. Neurochem.*, vol. 81, no. 6, pp. 1285–1297, 2002, doi: 10.1046/j.1471-4159.2002.00928. x.

[11] B. K. Gharia, J. Upadhyay, B. N. Suhagia, and S. A. Shah, "Current perspective of histone deacetylase inhibitors: A review," vol. 5, no. 3, pp. 108–122, 2018, doi: 10.18231/2394-2797.2018.0018.

[12] J. Ding *et al.*, "Design, synthesis and biological evaluation of coumarin-based N-hydroxycinnamamide derivatives as novel histone deacetylase inhibitors with anticancer activities," *Bioorg. Chem.*, vol. 101, p. 104023, 2020, doi: 10.1016/j.bioorg.2020.104023.

[13] M. Dokmanovic, C. Clarke, and P. A. Marks, "Histone deacetylase inhibitors: Overview and perspectives," *Mol. Cancer Res.*, vol. 5, no. 10, pp. 981–989, 2007, doi: 10.1158/1541-7786.MCR-07-0324.

[14] I. Koutsounas, C. Giaginis, E. Patsouris, and S. Theocharis, "Current evidence for histone deacetylase inhibitors in pancreatic cancer," *World J. Gastroenterol.*, vol. 19, no. 6, pp. 813–828, 2013, doi: 10.3748/wjg. v19.i6.813.

[15] P. A. Marks and W. S. Xu, "Histone deacetylase inhibitors: Potential in cancer therapy," *J. Cell. Biochem.*, vol. 107, no. 4, pp. 600–608, 2009, doi: 10.1002/jcb.22185.

[16] D. Al-Amily and M. H. Mohammed, "Design, synthesis and cytotoxicity study of primary amides as histone deacetylase inhibitors," *Iraqi J. Pharm. Sci.*, vol. 28, no. 2, pp. 151–158, 2019, doi: 10.31351/vol28iss2pp151-158.

[17] D. H. Al-Amily and M. Hassan, "Design, synthesis, and docking study of acyl thiourea derivatives as possible histone deacetylase inhibitors with a novel zinc binding group," *Sci. Pharm.*, vol. 87, no. 4, pp. 1–15, 2019, doi: 10.3390/scipharm87040028.

[18] O. M. Sagheer, M. H. Mohammed, J. S. Wadi, and Z. O. Ibraheem, "Studying the Cytotoxic Activity of Newly Designed and Synthesized HDAC Inhibitors Derivatives of Pentanoyl Anilide-5-Biguanide," *Macromol. Symp.*, vol. 401, no. 1, pp. 1–10, 2022, doi: 10.1002/masy.202100346.

[19] X.-J. Yang and S. Grégoire, "Class II Histone Deacetylases: from Sequence to Function, Regulation, and Clinical Implication," *Mol. Cell. Biol.*, vol. 25, no. 8, pp. 2873–2884, 2005, doi: 10.1128/mcb.25.8.2873-2884.2005.

[20] C. Seidel *et al.*, "Novel inhibitors of human histone deacetylases: Design, synthesis and bioactivity of 3-alkenoylcoumarines," *Bioorganic Med. Chem. Lett.*, vol. 24, no. 16, pp. 3797–3801, 2014, doi: 10.1016/j.bmcl.2014.06.067.

[21] M. A. Al-Haiza, M. S. Mostafa, and M. Y. El-Kady, "Synthesis and biological evaluation of some new coumarin derivatives," *Molecules*, vol. 8, no. 2, pp. 275–286, 2003, doi: 10.3390/80200275.

[22] Y. Luan, J. Li, J. A. Bernatchez, and R. Li, "Kinase and Histone Deacetylase Hybrid Inhibitors for Cancer Therapy," *J. Med. Chem.*, vol. 62, no. 7, pp. 3171–3183, 2019, doi: 10.1021/acs.jmedchem.8b00189.

[23] A. Benassi, F. Doria, and V. Pirota, "Groundbreaking anticancer activity of highly diversified oxadiazole scaffolds," *Int. J. Mol. Sci.*, vol. 21, no. 22, pp. 1–28, 2020, doi: 10.3390/ijms21228692.

[24] H. Rajak *et al.*, "2,5-Disubstituted-1,3,4-oxadiazoles/thiadiazole as surface recognition moiety: Design and synthesis of novel hydroxamic acid-based histone deacetylase inhibitors," *Bioorganic Med. Chem. Lett.*, vol. 21, no. 19, pp. 5735–5738, 2011, doi: 10.1016/j.bmcl.2011.08.022.

[25] H. D. Gurupadaswamy, V. Girish, C. V. Kavitha, S. C. Raghavan, and S. A. Khanum, "Synthesis and

evaluation of 2,5-di(4-aryloylaryloxymethyl)-1,3,4-oxadiazoles as anti-cancer agents," *Eur. J. Med. Chem.*, vol. 63, pp. 536–543, 2013, doi: 10.1016/j.ejmech.2013.02.040.

[26] W. S. Xu, R. B. Parmigiani, and P. A. Marks, "Histone deacetylase inhibitors: Molecular mechanisms of action," *Oncogene*, vol. 26, no. 37, pp. 5541–5552, 2007, doi: 10.1038/sj.onc.1210620.

[27] X. Zhang *et al.*, "A New Procedure for Preparation of Carboxylic Acid Hydrazides," no. 13, pp. 9471–9474, 2002.

[28] R. V Patel, P. Kumari, and B. Á. A. Á, "CHEMISTRY N -phenyl / benzothiazolyl acetamides as antimicrobial and antituberculosis agents," pp. 195–210, 2013, doi: 10.1007/s00044-012-0026-x.

[29] M. F. Tawfeeq and A. J. Qassir, "Synthesis, Characterization, and Antibacterial Evaluation of New Vanillic Acid Derivatives," vol. 29, no. 2, pp. 129–138, 2020.

[30] H. A. Sahib and M. H. Mohammed, "Synthesis and Preliminary Biological Activity Evaluation of New N- Substituted Phthalimide Derivatives\," vol. 29, no. 1, pp. 247–252, 2020.

[31] O. N. Wennas, M. H. Mohammed, and D. A. Abed, "Anti-Cancer Efficacy of 6 Mercaptopurine Loaded Biotinylated Cellulose Nanowhiskers," 2021, doi: 10.25258/ijddt.11.4.62.

[32] H. A. Sahib, Z. A. Dakhel, and M. K. Hadi, "Synthesis and Preliminary Antimicrobial Activity Evaluation of New Amide Derivatives of 2-aminobenzothiazole," pp. 2–5, 2021, doi: 10.25258/ijddt.11.4.23.

[33] B. A. Baviskar, M. R. Shiradkar, S. S. Khadabadi, S. L. Deore, and K. G. Bothara, "Note Synthesis of thiazolyltriazole substituted azetidinones as antimicrobial agents," vol. 50, no. March, pp. 321–325, 2011.

[34] B. E. L. Lauffer *et al.*, "Histone deacetylase (HDAC) inhibitor kinetic rate constants correlate with cellular histone acetylation but not transcription and cell viability," *J. Biol. Chem.*, vol. 288, no. 37, pp. 26926–26943, 2013, doi: 10.1074/jbc.M113.490706.